Following interfacial kinetics in real time using broadband evanescent wave cavity-enhanced absorption spectroscopy: a comparison of light-emitting diodes and supercontinuum sources

Lineke van der Sneppen,[a] Gus Hancock,[a] Clemens Kaminski,[bd] Toni Laurila,[b] Stuart R. Mackenzie,[a] Simon R. T. Neil,[a] Robert Peverall,[a] Grant A. D. Ritchie,*[a] Mathias Schnippering[c] and Patrick R. Unwin[c]

Received 12th August 2009, Accepted 13th November 2009
First published as an Advance Article on the web 24th November 2009
DOI: 10.1039/b916712a

A white light-emitting diode (LED) with emission between 420 and 700 nm and a supercontinuum (SC) source with emission between 450 and 2500 nm have been compared for use in evanescent wave broadband cavity-enhanced absorption spectroscopy (EW-BB-CEAS). The method is calibrated using a dye with known absorbance. While the LED is more economic as an excitation source, the SC source is superior both in terms of baseline noise (noise equivalent absorbances lower than 10^{-5} compared to 10^{-4} absorbance units (a.u.)) and accuracy of the measurement; these baseline noise levels are comparable to evanescent wave cavity ringdown spectroscopy (EW-CRDS) studies while the accessible spectral region of EW-BB-CEAS is much larger (420–750 nm in this study, compared to several tens of nanometres for EW-CRDS). The improvements afforded by the use of an SC source in combination with a high sensitivity detector are demonstrated in the broadband detection of electrogenerated Ir(IV) complexes in a thin-layer electrochemical cell arrangement. Excellent signal to noise is achieved with 10 μs signal accumulation times at a repetition rate of 600 Hz, easily fast enough to follow, in real time, solution kinetics and interfacial processes.

1 Introduction

The use of cavity-enhanced techniques such as cavity ringdown spectroscopy (CRDS) and cavity-enhanced absorption spectroscopy (CEAS) is well-established in the gas phase and is now a rapidly developing field for both liquid phase and evanescent wave studies, where analytes which have broadband spectra that exhibit little or no vibronic structure must be probed. The sensitive and selective detection of such species therefore relies upon combining broadband (BB) light sources with optical enhancement cavities.

CRDS is perhaps the most commonly used optical cavity technique and is based upon measuring the exponential decay rate, or ringdown time, τ, of the intensity of a light field in a cavity. The time τ is reduced from its empty cavity value in proportion to the frequency-dependent absorption coefficient of any analyte in the cavity; the basis of the technique's sensitivity arises from the large optical path lengths possible and the fact that these time domain measurements are unaffected by laser intensity fluctuations.[1,2]

However, despite its popularity in studies with both pulsed and continuous wave (cw) laser systems there have been relatively few CRDS studies using truly broadband sources. For example, while broadband cavity ringdown spectroscopy (BB-CRDS) measurements were pioneered as early as 1996,[3] the full potential of BB-CRDS was not explored further until much more recently. Exploratory BB-CRDS studies include the use of a Xe arc lamp and a combination of Fourier transform spectroscopy and phase-shift CRDS[4] and the use of an optical frequency comb for excitation over a wavelength region of 790–850 nm.[5] Recently, the feasibility of using a supercontinuum (SC) source in conjunction with a fast-gated intensified CCD camera has been demonstrated.[6]

CEAS is analogous to CRDS in that the measurement sensitivity is also increased by confining the analyte within the optical cavity formed by two (or more) high reflectivity mirrors.[7] In CEAS, however, the absorption is measured by integrating the total signal transmitted through an optical cavity[8–11] and the sensitivity is dependent on light source stability and the accuracy with which small intensity variations on the transmitted signal can be measured. In addition, CEAS requires a reliable calibration procedure in order to determine the baseline optical losses of the system; this baseline calibration is inherent in the CRDS measurements. Despite this drawback, CEAS is still an attractive alternative to CRDS as it is experimentally less demanding.

In the first demonstration of CEAS using an incoherent broadband (IBB) light source (dubbed IBB-CEAS), an absorption spectrum of jet cooled azulene was measured over a spectral range of 493–578 nm.[12] Other gas phase IBB-CEAS applications include the *in situ* detection of atmospheric trace gases such as NO_3,[13] NO_2 and glyoxal,[14] the development of Fourier transform

[a]*Department of Chemistry, Physical and Theoretical Chemistry Laboratory, University of Oxford, South Parks Road, Oxford, UK OX1 3QZ. E-mail: grant.ritchie@chem.ox.ac.uk; Fax: +44(0)1865 275410; Tel: +44(0)1865 285723*
[b]*Department of Chemical Engineering, University of Cambridge, Pembroke Street, Cambridge, UK CB2 3RA*
[c]*Department of Chemistry, University of Warwick, Gibbet Hill Road, Coventry, UK CV4 7AL*
[d]*School of Advanced Optical Technologies, Max Planck Institute for the Science of Light, Erlangen, Germany*

IBB-CEAS for the measurement of oxygen and water vapour[15] and the use of light-emitting diodes (LEDs) as light sources.[16–20] SC radiation, generated by non-linear interactions within optical fibres, provides exciting new opportunities for chemical sensing applications[21] combining extremely broad bandwidths[22] with high power and laser-like beam properties. Recently, BB-CEAS detection using an SC source in combination with narrow-band high reflectivity mirrors has been demonstrated.[23] In another study using an SC source, a ring cavity was constructed using two Pellin–Broca retroreflecting prisms[24] allowing for the use of the full wavelength range of the SC source (500–1750 nm). BB-CEAS is especially promising for application in condensed phase and interfacial studies, where species tend to exhibit broad, congested absorption features, and liquid phase IBB-CEAS using intra-cavity cuvettes has been demonstrated using both a Xe arc lamp[25] and LEDs;[26] IBB-CEAS has also been used as a detector in liquid chromatography.[27]

Two recent studies have coupled BB-CEAS with the use of evanescent waves (EWs) for the purpose of investigating interfacial phenomena. Ruth and Lynch used a Xe arc lamp to investigate thin dry films of metallo-porphyrins deposited from solution at the silica–air interface.[28] Some of the present authors have, in parallel, been developing a rapid variant of EW-BB-CEAS utilizing an SC source in order to explore interfacial kinetic processes in real time[29] to complement their previous interfacial EW-CRDS studies.[30–33] The superior spectral irradiance of the SC source greatly reduces the integration time necessary to achieve adequate signal to noise levels, permitting much higher spectral acquisition rates.

The present study aims to develop a reliable liquid phase EW-BB-CEAS experiment based on both LED and SC sources. In order to extract absolute absorbance values from the EW-BB-CEAS spectra, a convenient *in situ* calibration method using a dye of well-known absorbance has been used. The baseline noise levels and errors obtained for this calibration are used to demonstrate the performance of both systems while measuring static samples. The assessment of the performance in this way is important in itself, but also a pre-requisite for understanding the response of EW-BB-CEAS to evolving sample concentrations; this scenario is demonstrated in the application of liquid phase EW-BB-CEAS to the study of real-time fast interfacial kinetics, using the most sensitive implementation of EW-BB-CEAS, *i.e.* with SC source excitation.

2 Experimental

The experimental arrangement (shown in Fig. 1) uses cavities constructed using broadband mirrors (of reflectivity R = 0.9985–0.9998 between 400 and 800 nm, 500 mm radius of curvature or $R = 0.99 \pm 0.005$ between 420 and 640 nm, 200 mm radius of curvature) from Layertec (Mellingen, Germany). These mirror sets were combined to form optical cavities with mean mirror reflectivities of 99.9, 99.45 and 99%. An absorption spectrum of the mirrors as recorded on a Varian Cary 100 UV-Vis double-beam spectrometer is shown in Fig. 2 upper panel. While variations in mirror transmission are observed for the 99% mirror between 450 and 550 nm, the spectrometer is not sensitive enough to detect such variations for the 99.9% mirror.

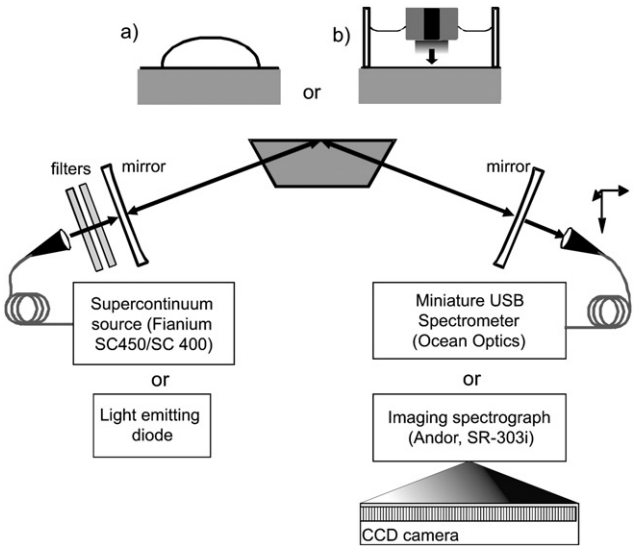

Fig. 1 Schematic of the experimental arrangement. Light from either an SC source or LED is injected into a folded optical cavity formed by two highly reflective concave mirrors and the total internal reflection surface of a custom Dove prism onto which either a drop of sample is placed (inset (a)) or an electrochemical cell is constructed (inset (b)). Light transmitted by the cavity is dispersed and detected using a spectrometer.

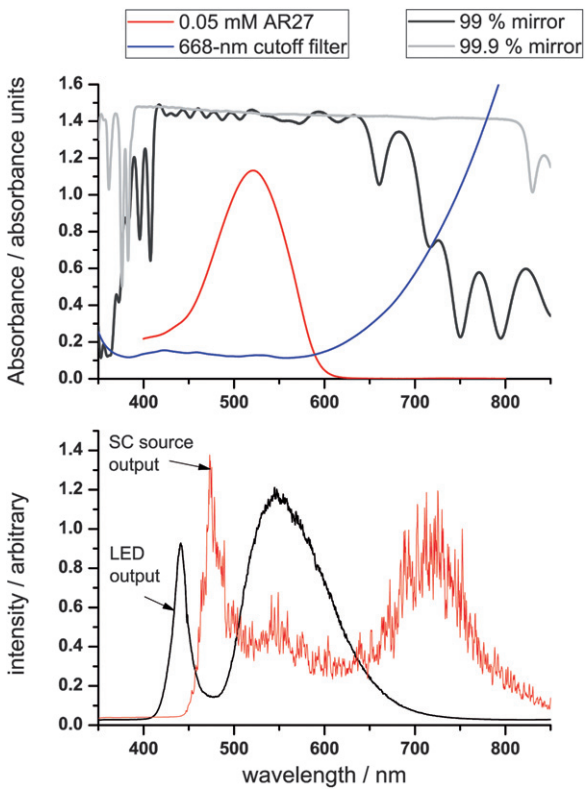

Fig. 2 Upper panel: absorbance spectrum of 0.05 mM Acid Red 27 in water (the calibration dye) together with the absorption spectrum of the two different mirrors. Lower panel: the output spectra of the LED and SC450-4 sources (the intensity was re-scaled for convenience). Note that the spikes on the spectrum of the SC source are reproducible spectral features.

A custom-made 70° Dove prism (Tower Optical, Boynton Beach, FL) is situated within the optical cavity and is used at normal incidence; reflection losses at intra-cavity surfaces are reduced with a broadband anti-reflection coating ($R \leq 0.0025$ between 450 and 650 nm). Scattering or absorption within the prism material (Heraeus Suprasil 911) is reduced by minimizing the prism dimensions and the single-pass path length through the prism is 18.8 mm. The entrance and exit faces are polished to a flatness of $\lambda/10$ at 632.8 nm while the total internal reflection (TIR) face is polished to a flatness of $\lambda/2$.[34] For experiments testing the performance of the LED and SC sources the cavity length was minimized and maintained within the range 72–78 mm. In order to accommodate a thin-layer electrochemical cell on top of the prism for the kinetics measurements, the small prism was replaced by a larger (33 mm path length), uncoated prism (Apex Services) in a 15 cm long cavity.

The LED used here is a 1 W Luxeon Star/o LED (LumiLEDs, San Jose, CA) with emission between 420 and 650 nm (Fig. 2, lower panel), and a beam divergence of 10°. Other than the use of an appropriate heat-sink, no attempts were taken to temperature-stabilize the LED as the emission spectrum did not change significantly over several hours. Additional collimating lenses were used in an effort to minimize the footprint of the LED at the TIR interface. Since the source is broadband and the optics are not achromatic, a variety of image planes are formed in the cavity and the time-averaged footprint of the excitation source (corresponding to the sampling area) at the TIR face will be larger than for a monochromatic source.[35] In addition, since the radius of curvature of the mirrors used for the three cases differ but the length of the cavity remains the same, the footprints at the TIR face will be different for each of the three cavities. Using highly dispersive samples, the footprints were estimated to have areas of 56, 46 and 32 mm^2 for the $R = 0.99$, 0.9945 and 0.999 cavity, respectively. A helium-neon laser which was carefully overlapped with the LED beam path was used for alignment of the cavity.

The SC source used in this study for comparison with LED excitation was a Fianium SC450-4 (Fianium Ltd., Southampton, UK) delivering a total emission of 4 W between 450 and 2500 nm; a slightly different SC source (the blue-enhanced Fianium SC400-2 with 2 W emission between 400 and 2500 nm) was used for the kinetic experiments. Intensity fluctuations on both Fianium sources for a one-second measurement are typically 0.5–1% (Fig. 2, lower panel shows the SC450-4 output spectrum). The output of the SC source was filtered using cold mirrors and suitable filters, *e.g.* a Comar 668 GK 50 short-pass filter (Fig. 2, upper panel). The randomly polarized output of the SC source was passed through a polarizer consisting of a stack of Brewster plates to ensure that the radiation incident upon the cavity had predominantly p-polarization; the footprints at the TIR interface were in the range of 6–8 mm^2, markedly smaller than for the LED.

The detector used for the comparison of the LED and the SC source was an Ocean-Optics USB 2000 + Czerny–Turner-type spectrometer (wavelength range 400–850 nm), and light was coupled into the spectrometer using a fibre with a 100 μm core and a fibre coupler of either NA = 0.25 or 0.50. All spectra were acquired in a time of 1 s. In order to fully utilize the superior sensitivity of the SC source (see later), the compact Ocean-Optics spectrometer was replaced with a faster and more sensitive spectrometer for recording the interfacial electrogeneration of Ir(IV) complexes in a thin-layer electrochemical cell arrangement.[29] A fibre-coupled Andor Shamrock SR-303i imaging spectrometer (wavelength range 533 nm centered at 546 nm, 150 lines per millimetre grating, blazed for 600 nm, 50 μm slit width), attached to a cooled CCD camera (Andor iXon, 512 × 512 pixels) has been used for this purpose. The 50 μm slit width was chosen to provide a spectral resolution of *ca.* 4 nm, significantly narrower than any spectral feature. Data were acquired over time periods of both 10 ms and 10 μs with vertical (spatial) binning performed either off-line (10 ms exposures) or on-chip (10 μs exposures).

The dyes used for calibrating and comparing the performance of the LED and SC sources were the negatively charged Acid Red 27 (AR27, purity 90%) and K_2IrCl_6, respectively (both obtained from Sigma-Aldrich, Germany). Measurements were performed covering the TIR footprint on the prism with a 40 μl drop of MilliQ water (Millipore), after which a background spectrum was taken. Concentrations were changed by adding and mixing 10 μl aliquots of aqueous solutions of 1 mM AR27 or 10 mM $[IrCl_6]^{2-}$ in this drop. No evaporation of the solvent was observed on the time-scales of the experiments, and between measurements, the prism surface was cleaned *in situ* using concentrated sulfuric acid, MilliQ water and methanol. The EW-BB-CEAS signals for both species are compared with single-pass absorbance spectra obtained using standard 1 cm cuvettes; the absorbance spectrum of a 0.05 mM aqueous solution of AR27 dye is shown in Fig. 2, upper panel, for illustrative purposes.

A thin-layer (100 μm) electrochemical cell was created above the TIR interface by positioning a 2 mm diameter Pt disk (working) electrode at a height of 100 μm above the prism. The cell contained a solution of 10 mM $[IrCl_6]^{3-}$ in 0.1 M KNO_3 (aq) as a supporting electrolyte. $[IrCl_6]^{2-}$ was electro-generated by stepping the potential of the working electrode from +0.4 to +1.0 V *vs.* a Ag/AgCl reference electrode for 60 s after which the potential was stepped back to +0.4 V. Calibration for these studies was provided by recording spectra of known Ir(IV) solutions.

3 Results and discussion

3.1 Performance of LED and SC sources in EW-BB-CEAS: static samples

For CEAS measurements, it can be shown in general that the absolute absorbance follows from the measured cavity transmission *via*:

$$\alpha_{anal} l = 2.303 \varepsilon C l = \left(\frac{I_0}{I} - 1\right)(1 - R) \quad (1)$$

where ε is the decadic molar extinction coefficient in M^{-1} cm^{-1}, α_{anal} is the absorption coefficient of the analyte, C is the concentration in M, l is the optical path length through the sample and R is the geometric mean of the mirror reflectivities. I_0 and I are the measured transmitted intensities without and with absorber on the TIR face, respectively. In gas phase experiments, the optical losses are normally dominated by the mirror transmission (other losses being scattering and diffraction losses) and the path length is enhanced by a factor of $(1 - R)^{-1}$. Knowledge

of the mirror reflectivity as a function of wavelength is therefore sufficient for extracting absolute absorbance values from the CEAS data. However, in EW-CEAS scattering losses at the entrance and exit faces of the intra-cavity prism as well as scattering and absorption in the prism itself exist, and thus must be determined. We therefore define a cavity enhancement factor CEF (to be experimentally determined) by the following equation:

$$\mathrm{CEF} = \frac{\left(\frac{I_0}{I} - 1\right)}{2.303\,\varepsilon Cl} \qquad (2)$$

To determine the wavelength-dependent CEFs, we measure the EW-BB-CEAS spectrum for four different concentrations (0.2, 0.33, 0.43 and 0.5 mM) of AR27: a negatively charged test dye, which we assume does not adsorb to the negatively charged surface. CEFs were found for a range of wavelengths by linear regression of plots of $(I_0/I - 1)$ *versus* C (eqn (2)). The ε values were determined using single-pass absorption spectroscopy, and we assume l to be the effective thickness, *i.e.* the path length that in a conventional transmission geometry would yield the same degree of absorption.[36,37] The effective thickness extends to infinity at the critical angle and care has been taken to ensure that the experiments are conducted some way from this condition (the angle of incidence is 70° compared with a critical angle of between 65 and 66° over the wavelength range used here). The effective thickness, and therefore the sensitivity with which small absorptions can be detected, depends upon wavelength and polarization, and example calculated values are given in Table 1. In order to make quantitative measurements of an aqueous solution of K_2IrCl_6 using EW-BB-CEAS, the $(I_0/I - 1)$ spectra are divided by 2.303(CEF), which then gives the spectrum of K_2IrCl_6 in absorbance units, εCl.

Examples of CEF values obtained with the LED and the SC sources in combination with the 99%, and 99.9% cavity are shown in the lower panels of Fig. 3 and Fig. 4, respectively, and have been determined using the calibration procedure described above. Clear structure in the CEF due to mirror reflectivity variations and additional scatter losses can be seen as a function of wavelength. For example, in the SC source data for the 99.9% cavity the CEF values are ~650 in the red and ~450 in the blue (where scattering losses are higher). The alignment of the optical cavities is more straightforward using the SC source, and generally slightly higher CEF values are obtained for a given mirror set. We note that this could be a result of the (relatively) poor collimation of the LED, which makes it more problematic for the cavity to contain the LED light rays after many passes: a situation potentially exacerbated by scattering from the prism surfaces. The measured CEF values are found to be dependent on day-to-day variations in the alignment: in the case of SC source working with the 99.9% mirrors, relatively large differences (sometimes up to 50%) are observed, following seemingly identical alignment procedures. This reinforces the need for the type of *in situ* calibration described here.

Table 1 Effective thicknesses calculated according to ref. 36 for different polarizations at selected wavelengths and a TIR angle of 70°

	Effective thickness/nm		
Wavelength/nm	p-pol.	s-pol.	random pol.
450	852	712	782
500	996	834	915
538	1095	919	1007
600	1295	1090	1192

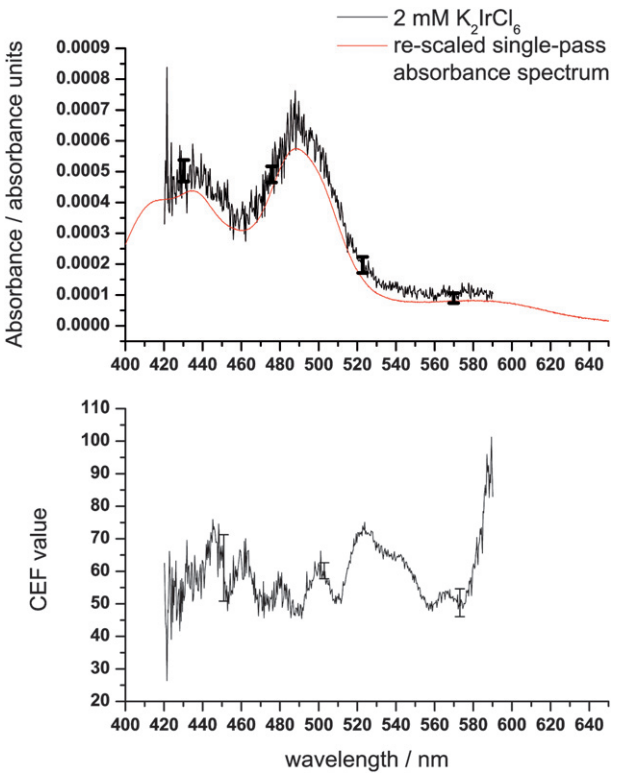

Fig. 3 Lower panel: the CEF values as a function of wavelength for the LED with the cavity of 99% mirror reflectivity. Upper panel: A spectrum (measurement time: 1 s) of 2 mM K_2IrCl_6 in water measured using the LED and after calibration using the CEF values obtained for AR27. Representative error bars obtained from the standard error of the predicted absorbance value as obtained from the calibration procedure are shown. An overlay with a re-scaled single-pass absorbance measurement is also shown.

In order to assess the performance of the two sources in relation to the cavities of different finesse the AR47 calibrations described above have been repeated in a series of three separate experiments for each cavity – source combination, each yielding a regression line based on twelve data points and three different values of I_0. The standard error for predicted absorbance values for all concentration values can be extracted from this regression, and an estimate of the baseline noise level is obtained from the EW-BB-CEAS calibration measurements. The standard errors and baseline noise levels for the three different cavities and the two sources are shown in Table 2. Clearly, the LED performs better when coupled with the lowest finesse cavity, and this is perhaps a reflection of the lower power reaching the detector and more problematic nature of the LED/cavity alignment. Conversely, the best choice in the case of the SC source would be the 99.9% cavity.

Absolute absorbance spectra (where absorbance is defined as εCl) of K_2IrCl_6 were obtained by dividing the measured spectra

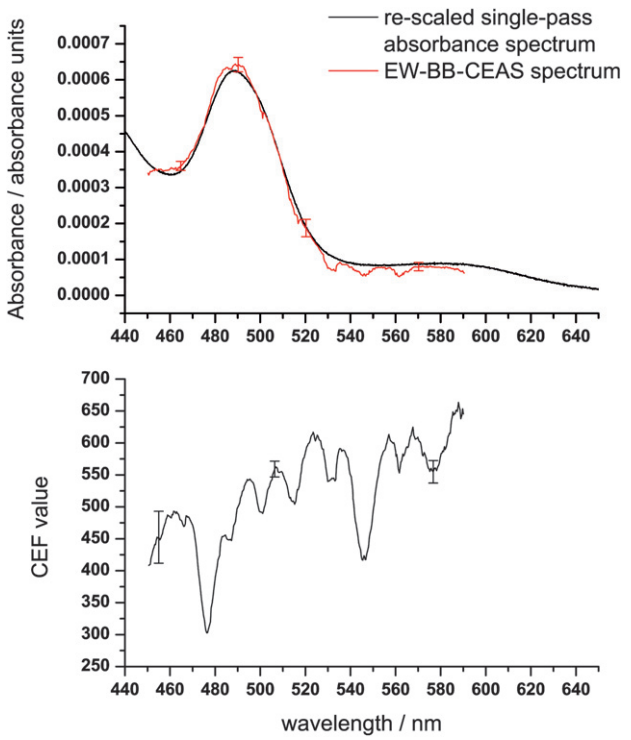

Fig. 4 Lower panel: the CEF values as a function of wavelength for the SC source with the cavity of 99.9% mirror reflectivity. Upper panel: A spectrum (measurement time: 1 s) of 2 mM $[IrCl_6]^{2-}$ in water after calibration with AR27 together with an overlay of a re-scaled single-pass absorbance measurement. Representative error bars obtained from the standard error of the predicted absorbance value as obtained from the calibration procedure are shown.

Table 2 Baseline noise levels and standard errors for the predicted absorbance for all concentrations as obtained from the regression lines of the calibration measurements

Cavity mirror reflectivity (%)	Light source	Baseline noise/10^{-4} (a.u.)	Standard error/10^{-4} (a.u.)
99	LED	0.3–1.0	0.2–0.5
	SC	0.2–0.3	0.5–0.6
99.45	LED	0.8–1.8	0.3–1.0
	SC	0.2–0.7	0.5–1.5
99.9	LED	1.0–4.0	0.8–2.5
	SC	0.1–0.4	0.1–0.2

by 2.303(CEF). Spectra of a concentration of 2 mM K_2IrCl_6 recorded using both the LED with the 99% cavity and the SC source with the 99.9% cavity are shown in the upper panels of Fig. 3 and Fig. 4 respectively. The figures also show the spectrum as determined from a single-pass absorption measurement, where data have been re-scaled taking into account the concentration difference and the effective thickness through the sample according to Table 1 and ref. 36. The extracted absorbance values deviate by less than 2 standard deviations (*i.e.* the 95% confidence interval of the regression) from the re-scaled single-pass measurement, and the processed spectrum is a good representation of the single-pass measurements. Baseline noise differs across the spectrum; at 460 and 570 nm the baseline noise is 1×10^{-4} and 3×10^{-5} absorbance units (a.u.) for the LED with the 99% cavity; for the SC source and the 99.9% cavity the baseline noise is 4×10^{-5} and 1×10^{-5} a.u. across the same region. The error estimates presented in both Fig. 3 and Fig. 4 reflect the statistical uncertainties of the measurement ascertained through the calibration procedure. Furthermore, we find that although they fall within the error bounds on the processed data, re-scaled (for effective thickness and concentration) single-pass data consistently underestimate the level of absorbance in the K_2IrCl_6 measurements. One possible explanation for this could lie in our assumption that the experiments probe a homogeneous bulk absorption.

Deviations in the CEF values, which reflect changes in mirror reflectivity, are larger with the 99.9% mirror set leading to large dips in the raw SC source spectra which are not completely corrected for by the calibration procedure. As a consequence of this, features in the calibrated spectra are present with a magnitude of 8×10^{-6} a.u. between 460 and 520 nm, and as large as 2×10^{-4} a.u. in the red region of the spectrum. Excluding mirror-related features which only show up at regular and reproducible intervals in the spectrum and which ideally would be mitigated by the calibration, the noise on the SC source EW-BB-CEAS spectrum was lower than 5×10^{-6} a.u., comparable or better than equivalent EW-CRDS arrangements.[30,34,37–44] In previous studies using narrow-band high reflectivity mirrors in combination with SC source excitation,[20,29] mirror-related features are absent in BB-CEAS measurements, and more favorable baseline noise levels and sensitivities are obtained. Therefore, as a consequence of long term experimental fluctuations, there is a play-off between greater specificity (where a longer wavelength coverage is desired) with the need for broadband mirrors, and sensitivity (which is better for narrow-band mirrors).

3.2 Using EW-BB-CEAS for following fast kinetics

Fig. 5 shows the signal (I_1) and reference (I_0) spectra obtained using the SC400 supercontinuum source and Andor detector with 10 mM $[IrCl_6]^{2-}$ solution in the cell above the prism. Both spectra represent 200 × 10 ms spectral averages (*i.e.*, a total accumulation time of 2 s each). The variations in the mirror reflectivity are clearly manifest in each spectrum with the transmitted light intensity greatest at the mirror reflectivity minima. The manufacturer's mirror reflectivity curve clearly shows these variations, too. The broader structure in the signal and reference spectra reflects the characteristics of the source itself.

The lower portion of Fig. 5 shows the cavity-enhanced absorption spectrum compared with a single-pass spectrum scaled for both the concentration difference and the spectral variation in the effective thickness. The ratio of the two provides the losses per round trip within the cavity (also shown, right hand scale), the reciprocal of which is the CEF which varies over this range from 200 to 800. Although the ripples in the mirror reflectivity are observed in the cavity losses, it is clear that the cavity loss spectrum is dominated by other losses which increase significantly towards the blue. These additional losses almost certainly arise from scattering both at the prism surfaces and within its bulk. As well as the ripples due to the mirror reflectivity, the cavity loss spectrum exhibits additional structure, noticeably peaks at 478 nm and 547 nm, but also other less prominent features. The origin of these is unclear but they appear

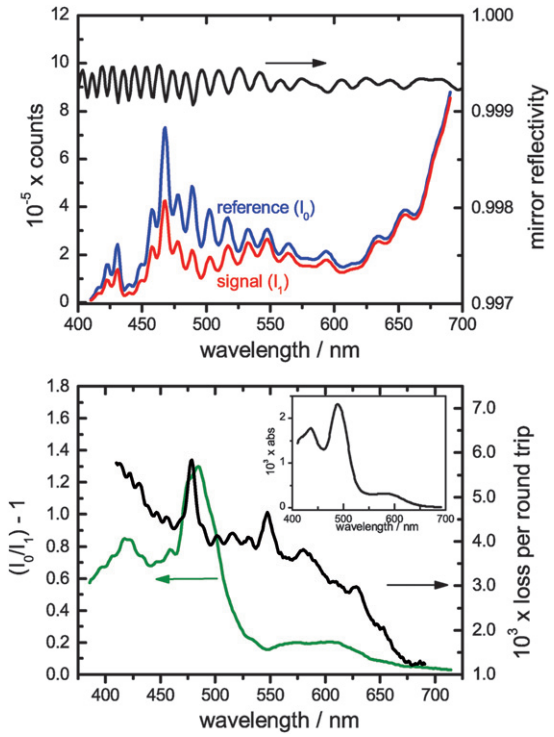

Fig. 5 Upper panel: Raw reference and signal spectra recorded for a sample of 10 mM Ir(IV) using the custom-coated broadband mirrors (reflectivity spectrum shown above). Lower panel: The extracted relative absorbance ($I_0/I_1 - 1$) spectrum for the Ir(IV) solution. The loss per round trip within the CEAS cavity was extracted by taking the ratio of this signal to the single-pass Ir(IV) spectrum of 2 mM Ir(IV) scaled for the (wavelength-dependent) effective thickness (inset).

in the data for both sets of experiments performed using the Layertec broadband mirrors. Since the light sources and detectors are different in each experiment, absorption or etaloning *within* the mirrors themselves appears the most likely source, though this merits further investigation.

One of the major advantages of incorporating an SC light source within a BB-CEAS arrangement is that the enhanced spectral irradiance it provides over other light sources permits the rapid acquisition of spectra with a high signal to noise ratio. This is illustrated in Fig. 6 which shows the temporal evolution of the spectrum (400–700 nm) of the interfacial (evanescent wave) region during the potential step generation of Ir(IV) within a 100 μm thin-layer electrochemical cell. The electro-oxidation of Ir(III) is achieved by stepping the working electrode from +0.4 V to +1.0 V relative to a Ag/AgCl reference electrode for 60 s following which it is stepped back to +0.4 V. The electro-generation and Ir(IV) diffusion kinetics have been modeled previously for a similar arrangement.[34] The interfacial spectrum was recorded with 10 μs accumulation times at a repetition rate of 606 Hz, limited by the data readout from the CCD array. For the purposes of Fig. 6 we have performed a six-shot running average on the data. The spectral and temporal cuts through the contour plot illustrate the high signal to noise ratio achievable even with such short acquisition times. The interfacial absorbance, the spectrum of which confirms that it arises from the Ir(IV) within the evanescent field (Fig. 6b), rises rapidly following

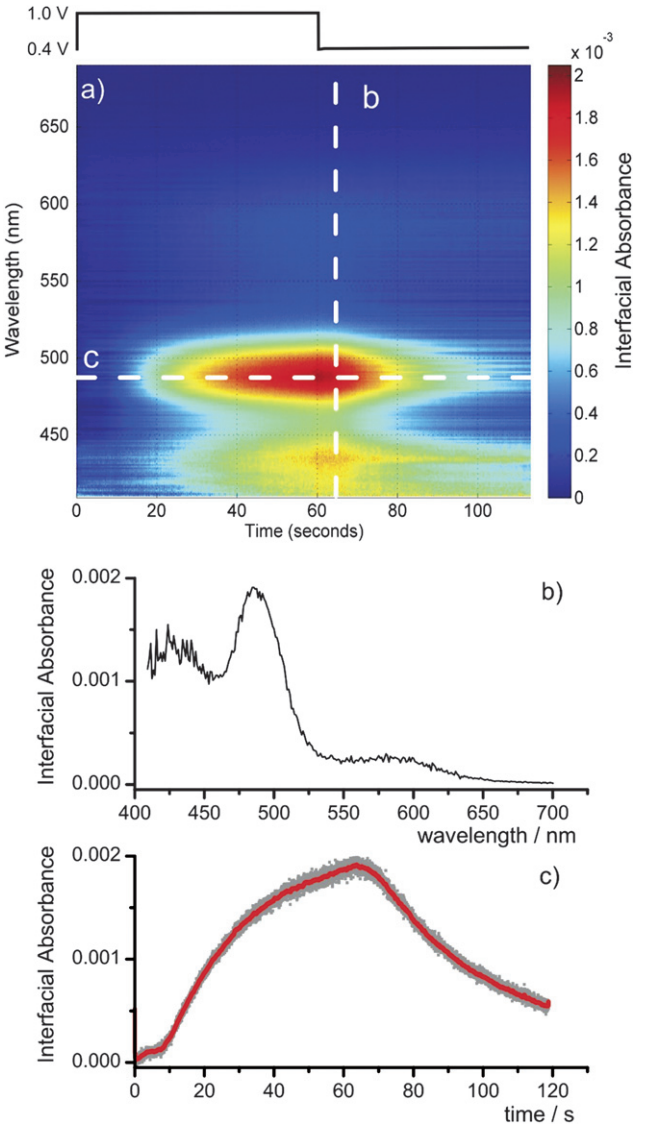

Fig. 6 (a) Contour plot of the interfacial absorbance spectrum as a function of time during the electrochemical generation of Ir(IV) in a 100 μm electrochemical cell. Data are recorded with 10 μs accumulation times at 606 Hz. (b) Spectral cut through the contour plot at 65 s, and (c) a temporal cut at 478 nm.

a delay of *ca.* 10 s during which time the Ir(IV) diffuses across the cell from the electrode to the silica surface. The absorbance approaches a maximum as the oxidation of the Ir(III) within the cell nears completion (Fig. 6c). Following the return step of the working electrode potential, the Ir(IV) is reduced once again and the interfacial absorbance drops.

From the data in Fig. 6 we can extract an effective minimum detectable absorbance of 3.9×10^{-5} a.u. at the peak of the absorbance spectrum. When scaled for the short accumulation times used in the acquisition of these data, this value is an improvement on that obtained in the comparison with the LED in Section 3.1, reflecting the improved detection arrangement. The sensitivity of this technique is ultimately limited by the stability of the SC source. A statistical analysis of the variation of intensity as a function of wavelength for 200 × 10 ms

accumulations suggests that this limit is highly wavelength dependent at $\leq 2 \times 10^{-6}$ a.u. for wavelengths above 650 nm, *ca.* 4×10^{-6} a.u. for 450–650 nm and rises steeply to 1.5×10^{-5} a.u. by 410 nm.

4 Conclusion

An EW-BB-CEAS experiment comprising of an LED, a plug-and-play USB spectrometer and two 99% cavity mirrors results in spectra with baseline noises lower than 10^{-4} absorbance units. By comparison, use of an SC source in combination with a higher finesse cavity formed from a 99.9% mirror set, allows baseline noise levels lower than 10^{-5} a.u. to be achieved. An *in situ* determination of cavity absorption values using a dye with well-known absorbance can be used for calibration; after this calibration procedure the precision of absolute absorbance values under optimal conditions, at the peak of the $[IrCl_6]^{2-}$ absorption, was found to be 5% for the LED and 3% for the SC source. Cavity enhancement factors were obtained from calculated EW effective thickness, and are of the order expected for the cavities used, but the accuracy of the CEF values has not been assessed. The broadband mirrors used in this study exhibit fringes in the reflectivity curve which result in periodically spaced spectral regions with increased baseline noise levels, an effect which was more pronounced in the more sensitive SC source EW-BB-CEAS spectra. The use of high-reflectivity narrow-band mirrors is likely to increase the sensitivity while compromising the broadband nature of the measurement.

An advantage of using SC source excitation rather than LED excitation is the fact that the source is collimated. One consequence of this is that the footprint at the TIR face of the prism is much smaller than in case of LED excitation, and a much smaller volume can be probed. Combining a high power SC source with a sensitive, fast readout detector permits the recording, with a good signal to noise ratio, of the full visible spectrum (400–700 nm) of an interfacial layer at rates $\geq$600 Hz with data accumulation times of only 10 μs. This is sufficient to follow fast kinetics in condensed phases in real time. Even under these challenging conditions, minimum detectable absorbances of $\leq 5 \times 10^{-5}$ a.u. are achievable. This methodology therefore provides a significant addition to the armoury of those interested in dynamical interfacial phenomena.

Acknowledgements

L.v.d.S. acknowledges The Netherlands Organisation for Scientific Research (NWO) for a Rubicon grant at the University of Oxford. T.L. acknowledges support from the Finnish Cultural Foundation and both S.R.M. and R.P. are grateful to the EPSRC for their Advanced Research Fellowships. C.F.K. acknowledges the EPSRC for support through a Platform grant EP/F028261/1.

References

1 *Cavity-Ringdown Spectroscopy: An Ultratrace-Absorption Measurement Technique*, ed. K. W. Busch and M. A. Busch, ACS Symp. Ser. 720, American Chemical Society, Washington, 1999.
2 *Cavity Ring-Down Spectroscopy: Techniques and Applications*, ed. G. Berden and R. Engeln, Wiley, Chichester, 2009.
3 R. Engeln and G. Meijer, *Rev. Sci. Instrum.*, 1996, **67**, 2708.
4 E. Hamers, D. C. Schram and R. Engeln, *Chem. Phys. Lett.*, 2002, **365**, 237.
5 M. J. Thorpe, K. D. Moll, R. J. Jones, B. Safdi and J. Ye, *Science*, 2006, **311**, 1595.
6 K. Stelmaszczyk, P. Rohwetter, M. Fechner, M. Queisser, A. Czyzsewski, T. Stacewicz and L. L. Woeste, *Opt. Express*, 2009, **17**, 3673.
7 P. K. Dasgupta and J.-S. Rhee, *Anal. Chem.*, 1987, **59**, 783.
8 A. O'Keefe, *Chem. Phys. Lett.*, 1998, **293**, 331.
9 A. O'Keefe, J. J. Scherer and J. B. Paul, *Chem. Phys. Lett.*, 1999, **307**, 343.
10 T. Gherman and D. Romanini, *Opt. Express*, 2002, **10**, 1033.
11 T. Gherman, D. Romanini, I. Sagnes, A. Garnache and Z. Zhang, *Chem. Phys. Lett.*, 2004, **390**, 290.
12 S. E. Fiedler, G. Hoheisel, A. A. Ruth and A. Hese, *Chem. Phys. Lett.*, 2003, **382**, 447.
13 D. S. Venables, T. Gherman, J. Orphal, J. C. Wenger and A. A. Ruth, *Environ. Sci. Technol.*, 2006, **40**, 6758.
14 R. A. Washenfelder, A. O. Langford, H. Fuchs and S. S. Brown, *Atmos. Chem. Phys.*, 2008, **8**, 7779.
15 A. A. Ruth, J. Orphal and S. E. Fiedler, *Appl. Opt.*, 2007, **46**, 3611.
16 S. M. Ball, J. M. Langridge and R. L. Jones, *Chem. Phys. Lett.*, 2004, **398**, 68.
17 T. Gherman, D. S. Venables, S. Vaughan, J. Orphal and A. A. Ruth, *Environ. Sci. Technol.*, 2008, **42**, 890.
18 M. Triki, P. Cermak, G. Mejean and D. Romanini, *Appl. Phys. B: Lasers Opt.*, 2008, **91**, 195.
19 T. Wu, W. Zhao, W. Chen, W. Zhang and X. Gao, *Appl. Phys. B: Lasers Opt.*, 2009, **94**, 85.
20 J. M. Langridge, S. M. Ball, A. J. L. Shillings and R. L. Jones, *Rev. Sci. Instrum.*, 2008, **79**, 123110.
21 C. F. Kaminski, R. S. Watt, A. D. Elder, J. H. Frank and J. Hult, *Appl. Phys. B: Lasers Opt.*, 2008, **92**, 367.
22 R. S. Watt, C. F. Kaminski and J. Hult, *Appl. Phys. B: Lasers Opt.*, 2008, **90**, 47.
23 J. M. Langridge, T. Laurila, R. S. Watt, R. L. Jones, C. F. Kaminski and J. Hult, *Opt. Express*, 2008, **16**, 10178.
24 J. P. S. Johnston and K. K. Lehmann, *Opt. Express*, 2008, **16**, 15013.
25 S. E. Fiedler, A. Hese and A. A. Ruth, *Rev. Sci. Instrum.*, 2005, **76**, 023107.
26 M. Islam, L. N. Seetohul and Z. Ali, *Appl. Spectrosc.*, 2007, **61**, 649.
27 L. N. Seetohul, Z. Ali and M. Islam, *Anal. Chem.*, 2009, **81**, 4106.
28 A. A. Ruth and K. T. Lynch, *Phys. Chem. Chem. Phys.*, 2008, **10**, 7098.
29 M. Schnippering, P. R. Unwin, J. Hult, T. Laurila, C. F. Kaminski, J. M. Langridge, R. L. Jones, M. Mazurenka and S. R. Mackenzie, *Electrochem. Commun.*, 2008, **10**, 1827.
30 M. Mazurenka, L. Wilkins, J. V. Macpherson, P. R. Unwin and S. R. Mackenzie, *Anal. Chem.*, 2006, **78**, 6833.
31 M. Mazurenka, S. M. Hamilton, P. R. Unwin and S. R. Mackenzie, *J. Phys. Chem. C*, 2008, **112**, 6462.
32 H. V. Powell, M. Schnippering, M. Mazurenka, J. V. Macpherson, S. R. Mackenzie and P. R. Unwin, *Langmuir*, 2009, **25**, 248.
33 M. Schnippering, H. V. Powell, M. Zhang, J. V. Macpherson, P. R. Unwin, M. Mazurenka and S. R. Mackenzie, *J. Phys. Chem. C*, 2008, **112**, 15274.
34 L. van der Sneppen, J. B. Buijs, C. Gooijer, W. Ubachs and F. Ariese, *Appl. Spectrosc.*, 2008, **62**, 649.
35 S. E. Fiedler, A. Hese and U. Heitmann, *Rev. Sci. Instrum.*, 2007, **78**, 073104.
36 N. J. Harrick, *Infrared reflection spectroscopy*, Harrick Scientific Corporation, New York, USA, 1987.
37 L. van der Sneppen, C. Gooijer, W. Ubachs and F. Ariese, *Sens. Actuators, B*, 2009, **139**, 505.
38 J. D. Fisk, R. Batten, G. Jones, J. P. O'Reilly and A. M. Shaw, *J. Phys. Chem. B*, 2005, **109**, 14475.
39 W. B. Martin, S. Mirov, D. Martyshkin and R. Venugopalan, *J. Biomed. Opt.*, 2005, **10**, 024025.
40 F. Li and R. N. Zare, *J. Phys. Chem. B*, 2005, **109**, 3330.
41 M. A. Everest, V. M. Black, A. S. Haehlen, G. A. Haveman, C. J. Kliewer and H. A. Neill, *J. Phys. Chem. B*, 2006, **110**, 19461.
42 H.-F. Fan, C.-Y. Hung and K.-C. Lin, *Anal. Chem.*, 2006, **78**, 3583.
43 J. D. Fisk, M. Rooth and A. M. Shaw, *J. Phys. Chem. C*, 2007, **111**, 2588.
44 X. Wang, M. Hinz, M. Vogelsang, T. Welsch, D. Kaufmann and H. Jones, *Chem. Phys. Lett.*, 2008, **467**, 9.